Available online at www.sciencedirect.com
ScienceDirect
Nuclear Medicine and Biology 38 (2011) 885–896
NUCLEAR MEDICINE AND BIOLOGY
www.elsevier.com/locate/nucmedbio

Evaluation of ^{111}In labeled antibodies for SPECT imaging of mesothelin expressing tumors

Ripen Misri[a], Katayoun Saatchi[a], Sylvia S.W. Ng[a,b], Ujendra Kumar[a], Urs O. Häfeli[a,*]

[a]Faculty of Pharmaceutical Sciences, University of British Columbia, Vancouver, BC, Canada V6T 1Z3
[b]Advanced Therapeutics, British Columbia Cancer Agency, Vancouver BC V5Z 1G1

Received 27 September 2010; received in revised form 1 February 2011; accepted 27 February 2011

Abstract

Introduction: Mesothelin is expressed in many cancers, especially in mesothelioma and lung, pancreatic and ovarian cancers. In the present study, we evaluate ^{111}In labeled antimesothelin antibodies as an imaging bioprobe for the SPECT imaging of mesothelin-expressing tumors.
Methods: We radiolabeled the antimesothelin antibodies mAbMB and mAbK1 with ^{111}In using the p-SCN-bn-DTPA chelator. The immunoreactivity, affinity (K_d) and internalization properties of the resulting two ^{111}In labeled antibodies were evaluated in vitro using mesothelin-expressing A431K5 cells. The biodistribution and microSPECT/CT imaging studies with ^{111}In labeled antibodies were performed in mice bearing both mesothelin positive (A431K5) and mesothelin negative (A431) tumors.
Results: In vitro studies demonstrated that ^{111}In-mAbMB bound with a higher affinity (K_d=3.6±1.7 nM) to the mesothelin-expressing A431K5 cells than did the ^{111}In-mAbK1 (K_d=29.3±2.3 nM). ^{111}In-mAbMB was also internalized at a greater rate and extent into the A431K5 cells than was the ^{111}In-mAbK1. Biodistribution studies showed that ^{111}In-mAbMB was preferentially localized in A431K5 tumors when compared to A431 tumors. At the low dose, the peak A431K5 tumor uptake of 9.65±2.65% ID/g (injected dose per gram) occurred at 48 h, while at high dose tumor uptake peaked with 14.29±6.18% ID/g at 72 h. Non-specific localization of ^{111}In-mAbMB was mainly observed in spleen. ^{111}In-mAbK1 also showed superior localization in A431K5 tumors than in A431 tumors, but the peak uptake was only 3.04±0.68% ID/g at 24 h. MicroSPECT/CT studies confirmed better visualization of A431K5 tumors with ^{111}In-mAbMB, than with ^{111}In-mAbK1.
Conclusion: SPECT imaging of mesothelin expressing tumors was demonstrated successfully. Our findings indicate that the antimesothelin antibody mAbMB has the potential to be developed into a diagnostic agent for imaging mesothelin-expressing cancers.

Keywords: Radiolabeled antibody; Mesothelin; Biodistribution; In-111; SPECT/CT

1. Introduction

Malignant mesothelioma, pancreatic cancer and ovarian cancer are all characterized by low survival rates. Pancreatic cancer has the highest mortality of all cancers, with a 5-year survival rate of only 5%, while those of mesothelioma and ovarian cancer are also bad with 9% and 30%, respectively [1,2]. These low survival rates can be attributed to late diagnosis and the cancers' propensity for early metastasis, both of which significantly reduce the chance of a cure. Early detection can increase the survival rates by allowing the identification of tumors, at a time when they are still amenable to surgical resection or other therapeutic approaches. Imaging has a pivotal role to play in the detection and treatment planning of these cancers [3–5]. Better imaging of the tumor sites would also permit more accurately targeted drug or radiation delivery for subsequent management of the disease [6]. Although improved imaging methods are needed to assist in detection and treatment, few agents have been designed to image the molecular targets expressed by these cancers [7–10].

A number of studies have shown that mesotheliomas, pancreatic and ovarian cancers overexpress mesothelin, a cell surface glycoprotein which can potentially be useful as a target for development of novel imaging and treatment strategies [11–14]. Mesothelin, a 40 kDa glycosylphosphatidyl-inositol (GPI) anchored cell surface glycoprotein, is expressed at low levels by a restricted set of normal adult

* Corresponding author. Tel.: +1 604 822 7133; fax: +1 604 822 3035.
E-mail address: uhafeli@interchange.ubc.ca (U.O. Häfeli).

0969-8051/$ – see front matter © 2011 Elsevier Inc. All rights reserved.
doi:10.1016/j.nucmedbio.2011.02.013

tissues, but is overexpressed in 50-65% of mesotheliomas, ovarian cancers, pancreatic cancers, and some lung adenocarcinomas [13,15]. Overexpression of mesothelin has been associated with increased proliferation, migration, and tumor volume [16]. Mesothelin specific targeting for imaging and therapy thus holds great promise in the management of these cancers. One way to do this is to use monoclonal antibodies specific to tumor-associated antigens and use them as delivery vehicles for radionuclides to visualize or treat tumors [17]. An antibody to mesothelin, when labeled with a radionuclide for imaging, would be valuable as a molecular imaging bioprobe, especially given its limited expression in normal tissues and high expression in specific cancers.

The first anti-mesothelin antibody mAbK1 (IgG1) was isolated from mice immunized with an ovarian cancer cell line [18]. Subsequently, Hassan et al. showed in a biodistribution study the targeting potential of ^{111}In-labeled mAbK1 in mice bearing mesothelin positive and mesothelin negative tumors [19]. Since then many new anti-mesothelin antibodies have been reported and become commercially available. However, there has not been much progress in the molecular imaging of mesothelin-expressing cancers, with only one recently published study using ^{64}Cu-radiolabeled antibody fragments for the PET imaging of mesothelioma in mice [9]. Onda et al. reported two new antibodies, mAbMB and mAbMN, and compared their anti-mesothelin affinity characteristics with the other available antibodies including mAbK1, showing that mAbMB (IgG2A) has the best affinity for mesothelin [11].

Our lab is interested in the imaging and potential treatment of mesotheliomas and pancreatic cancer with radiopharmaceuticals. For this purpose, we recently performed a biodistribution study with mAbK1 antibody radiolabeled with ^{99m}Tc (unpublished data). Using the direct labeling method [20], 0.2 mg of mAbK1 was radiolabeled with 90 MBq of ^{99m}Tc and then injected into SCID mice with mesothelin-expressing NCI-H226 tumors. The tumor uptake at 8 hours was only 0.8% ID/g showing a further decrease at subsequent time points. Compared to Hassan et al.'s reported 53% ID/g uptake in mesothelin-expressing A431K5 tumors with the ^{111}In-labeled mAbK1 antibody [19], this was very low. In the current study, we firstly sought to identify the reasons for this difference in tumor uptake by evaluating ^{111}In labeled mAbK1 (^{111}In-mAbK1) in the same A431K5 tumor model reported previously by Hassan et al. Secondly, with the aim of developing a radiotracer for imaging mesothelin-expressing tumors, we tested ^{111}In labeled mAbMB antibody (^{111}In-mAbMB) for its potential to selectively accumulate at a tumor site and to be imaged by SPECT/CT. We also compared the characteristics of ^{111}In-mAbMB to those of ^{111}In-mAbK1 in order to find the optimal one for imaging. Herein, we describe the radiolabeling of the mesothelin antibodies mAbMB and mAbK1 and report their immunoreactivity, affinity, internalization characteristics, and biodistribution. The SPECT/CT imaging properties of the two antibodies, which has not been reported previously, was also evaluated in tumor-bearing mice.

2. Materials and methods

2.1. Materials

All chemicals and reagents were purchased from Sigma-Aldrich (Oakville, Ontario, Canada). The mAbMB antibody was purchased from Rockland Immunochemicals (Gilbertsville, Pennsylvania, U.S.A.) and mAbK1 from Abcam (Cambridge, Massachusetts, U.S.A.). ITLC strips were obtained from Biodex (Cat# 150−771; Shirley, New York, U.S.A.). The cell culture media and supplements were obtained from Invitrogen (Burlington, Ontario, Canada). $^{111}InCl_3$ was obtained from MDS Nordion (Vancouver, British Columbia, Canada) and p-SCN-bn-DTPA from Macrocyclics (Dallas, Texas, U.S.A.). Ultracel 100K centrifugal filters were purchased from Millipore Corporation (Billerica, Massachusetts, U.S.A.). Reagents for electrophoresis were purchased from BIO-RAD Laboratories (Mississauga, Ontario, Canada). Activity measurements were carried out using a Packard Cobra II gamma counter (Perkin-Elmer, Waltham, Massachusetts, U.S.A.).

2.2. Radiolabeling

Antimesothelin antibodies mAbMB and mAbK1 were purified and buffer-exchanged into 0.1 M sodium bicarbonate, pH 8.5 using 100 kDa cut-off Ultracel centrifugal filters, and incubated on an Eppendorf shaker for 21 hours at room temperature with p-SCN-bn-DTPA in 0.1 M sodium bicarbonate at a molar ratio of 1:5. After 21 hours, unreacted DTPA (diethylene triamine pentaacetic acid) was removed by centrifugation through the centrifugal filters and antibody buffer-exchanged into 0.15 M ammonium acetate buffer, pH 5.5. For ^{111}In-labeling, $^{111}InCl_3$ (3.7 MBq/20 μg of antibody) was added to mAbMB and mAbK1 antibody, respectively, and incubated for 30 minutes on an Eppendorf shaker at room temperature. The radiolabeled antibodies were purified using the centrifugal filters and buffer-exchanged into phosphate buffered saline, pH 7.4 (PBS) for injection into mice or in vitro testing. Radiochemical purity was determined using ITLC-SG plates after DTPA challenge (0.05 M). Saline was used as the mobile phase. In this ITLC system, ^{111}In DTPA moves to R_f=1 and ^{111}In mAb to R_f=0. The number of DTPA molecules conjugated to the antibody was determined by trace labeling with $^{111}InCl_3$ [21].

2.3. Cell culture

A431K5 and A431 cell lines were generously provided by Dr. Ira Pastan (NCI, Bethesda, Maryland, U.S.A.) and Dr. Marcel Bally (Advanced Therapeutics, British Columbia Cancer Agency, Vancouver, Canada), respectively. Both cell lines were cultured in Dulbecco's Modified Eagle medium

supplemented with 10% fetal bovine serum, at 37°C in a humidified atmosphere in presence of 5% CO_2 as reported previously [19].

2.4. Determination of immunoreactivity

A cell binding assay was carried out to determine the immunoreactivity of ^{111}In-mAbK1 and ^{111}In-mAbMB [22]. Different concentrations (2×10^6 cells/ml to 10×10^6 cells/ml) of mesothelin-expressing A431K5 cells were incubated with 5 ng of ^{111}In-mAbK1 or ^{111}In-mAbMB on a rocker at 4°C for 2 hours. Following incubation, the cells were centrifuged for 5 minutes at 500 g, the supernatant was removed and the cells were washed 3 times with PBS containing 1% BSA and counted in a γ-counter to determine the total binding of ^{111}In-labeled antibody to A431K5 cells. Non-specific binding was determined in presence of excess unlabeled antibody (10 μg). Specific binding was calculated as the difference between total and non-specific binding to A431K5 cells. The immunoreactivities were calculated from the Y-intercept of the double reciprocal plot of fraction of the radioactivity specifically bound *vs*. the cell number.

2.5. Saturation binding - K_d and B_{max} determination

Radioligand saturation cell binding experiments were carried out for determination of the dissociation constant K_d and maximum number of binding sites B_{max} for ^{111}In-mAbMB and ^{111}In-mAbK1 [23]. The average number of mesothelin receptors present on A431K5 cells was calculated by conversion of the B_{max} values. Briefly, about 50,000 A431K5 cells/well were plated overnight in a 24 well plate. Adherent cells were then incubated in serum-free culture media with increasing concentrations (0–80 nM) of ^{111}In-antibody (mAbMB and mAbK1) in a total volume of 500 μl for 3 h at 4°C. The cells were then washed twice with ice-cold PBS to remove unbound radioactivity, dissolved in 0.1 M NaOH and analyzed in a γ-counter. Prism Version 5.0 software (GraphPad Software, San Diego, CA, USA) was used to fit the total binding values against the concentration of unbound radiolabeled antibodies, to a one-site saturation binding model. K_d and B_{max} were determined using this model by fitting only total binding, assuming that the amount of nonspecific binding was proportional to the concentration of radioligand.

2.6. Internalization of ^{111}In-labeled antibodies by A431K5 cells

To determine and compare the rate of internalization of ^{111}In-mAbMB labeled antibodies and ^{111}In-mAbK1 by A431K5 cells, an internalization assay was carried out [24]. Briefly, 1×10^6 A431K5 cells were incubated in 1 ml medium with 5 ng of ^{111}In-labeled antibody for 1 hour at 4°C in culture tubes. Centrifugation for 5 minutes at 200 g was carried out to remove the unbound antibody, followed by one wash with ice-cold PBS. The cells were then re-cultured with 1 ml of medium or counted on the γ-counter for determination of internalization at time 0. At 3, 6 and 18 hours, the internalized fraction was separated by treating with 1 ml acidic buffer (0.1 M acetic acid in 0.01 M PBS, pH 2.85) and pelletized by centrifuging for 5 minutes at 200 g. The supernatant comprising the membrane-bound fraction (acid labile) was separated and both fractions counted in a γ- counter.

2.7. Tumor uptake and biodistribution

Tumor uptake and biodistribution experiments were carried out in male C.B-17 SCID mice (Taconic, Germantown, New York, U.S.A.). Mice were injected with 8×10^6 A431K5 (mesothelin positive) cells in the nape of the neck and the same number of A431 cells (mesothelin negative) in the lower back. When tumors exceeded a size of 5 mm in diameter, four groups of mice (n=5) were injected intravenously with about 4 μg/740 kBq of ^{111}In-mAbMB and euthanized 24, 48, 72 and 96 hours later, all major organs removed and analyzed. Biodistribution of ^{111}In-mAbMB was similarly evaluated at 24 hours in one group of mice (n=3) not bearing any tumors.

Biodistribution of ^{111}In-mAbK1 was evaluated in 2 groups of mice (n=5) after injecting 740 kBq of ^{111}In-mAbK1 intravenously followed by euthanasia at 24 and 72 hours for collection of major organs. Additionally, biodistribution of ^{111}In-mAbMB antibody was also studied at a higher dose of between 7.4 to 10.1 MBq (50 μg/9.25 MBq) in two groups of mice (n=3) at 24 and 72 hours. To compare the extent of radioactivity localization in different organs and tumor, the ratio of radioactivity in different tissues and total blood (for the same weight) was determined. Animal experiments were carried out in accordance with the guidelines of the University of British Columbia's Animal Care Committee.

2.8. MicroSPECT/CT Imaging

MicroSPECT/CT imaging of mice bearing A431K5 and A431 tumors was performed after injection of ^{111}In-mAbMB at 24 (n=6), 48 (n=6) and 72 hours (n=3). In a parallel study, tumor-bearing mice (n=2) were injected with ^{111}In-mAbK1 and imaging was performed at 24, 48 and 72 hours. After injecting 7.4 to 10.1 MBq of activity, mice were anesthetized using isoflurane and acquisitions were performed on a GammaMedica Ideas X-SPECT system (North Ridge, California, U.S.A.). CT acquisitions consisted of 1024 projections acquired over 360° with a 70 kVp, 205 μA cone beam x-ray. Cobra Exxim software (Feldkamp filtered back projection cone beam software) was used to reconstruct the image at an isotropic voxel size of 0.155 mm. The SPECT images were acquired using a dual head system fitted with 1 mm aperture medium energy pinhole collimators set at an ROR of 77 mm. Energy windows (10%) were set over the 173 keV and 247 keV peaks. The total counts/scan for 24, 48 and 72 hour

acquisitions were 60,000-90,000, 45,000-65,000 and 40,000-50,000, respectively. GammaMedica-Ideas FLEX-SPECT software was used to reconstruct the data at an isotropic 1.17033 mm voxel size. After fusion of the SPECT and CT data, region of interest (ROI) analysis was carried out using AMIDE software (version 0.9.1) [25] to determine the target to non-target ratios (T/NT) for both A431K5 and A431 tumors and statistical significance calculated by student's t-test. Due to small sample size (n=2), statistical analysis was not carried out for ROI data of images obtained with ^{111}In-mAbK1.

2.9. Mesothelin expression in tumors

The verification of mesothelin protein expression in the harvested tumors was performed by Western blot using the anti mesothelin antibody mAbMB. A431K5 cells in culture flasks were washed with PBS and lysed in 1 ml of RIPA buffer [150 mM NaCl, 1% nonyl phenoxylpolyethoxylethanol, 0.5% Na deoxycholate, 0.1% Na dodecylsulfate, 50 mM Tris-HCl (pH 7.5), 1% protease inhibitor cocktail (Sigma)]. The cell lysates were centrifuged at 8,000 rpm (5223 g) for 10 min at 4 °C and the supernatant was collected. Tumor lysates were prepared by homogenizing frozen tumor (five A431K5 tumors K1-K5; five A431 tumors A1-A5) samples in 1 ml of ice-cold homogenization buffer [10 mM EGTA, 2 mM EDTA, 25 mM sucrose, Tris-HCl 20 mM (pH 7.5), 1% protease inhibitor cocktail], followed by sonication for 10 seconds. As spleen lysate (S) was also prepared to check for any cross reactivity by western blot analysis. A431K5 cell lysates were prepared and used as a positive control. The lysates were centrifuged at 11,000 rpm (9875 g) for 10 min at 4 °C and the supernatant was collected. Samples were prepared for electrophoresis in Laemmli sample buffer (Bio-Rad) containing 5% v/v of 2-mercaptoethanol (Bio-Rad). The samples were heated at 99 °C for 5 min, fractionated using SDS-polyacrylamide gel (12% gel), and then transferred onto a nitrocellulose Hy-Bond ECL membrane (Amersham Ltd. Oakdale, Ontario, Canada). The membrane was then processed for washing with 5% milk in Tris-Buffered Saline Tween-20 (TBST) for 1 h at room temperature (RT) followed by incubation with the anti-mesothelin antibody mAbMB in 5% BSA in TBST at 1:1000 dilution overnight at 4°C. Secondary antibody 1:5000 (horseshoe peroxidase-labeled goat antimouse IgG; Jackson ImmunoResearch Laboratories) was incubated for 1 h at RT followed by chemiluminescence detection using the ECL Western blotting detection kit (Amersham) according to the manufacturer's suggested protocol. Images were captured using an Alpha Innotech FluorChem 8800 gel box imager (Alpha Innotech Co., San Leandro, California, U.S.A.). The bands were quantified by densitometric analysis using FluorChem software (Alpha Innotech). As a loading control, the membrane was stripped and reprobed with monoclonal anti-β-actin antibody (Sigma).

2.10. Statistical analysis

Statistical analysis was carried out by Students t test using Origin version 7 for Windows. P values of each analysis were used to assess the significance of the data.

3. Results

3.1. Radiolabeling

^{111}In-labeling of both mAbK1 and mAbMB using the p-SCN-bn-DTPA chelator was consistently accomplished with labeling efficiencies of about 95% (94.78±0.63% for ^{111}In-mAbMB and 95.44±0.25% for ^{111}In-mAbK1). The average number of bound DTPA molecules was 2.6 per molecule of mAbK1 and 2.4 per molecule of mAbMB.

3.2. Immunoreactivity and saturation cell binding studies

The results of the immunoreactivity assay and saturation cell binding studies are summarized in Table 1. Both ^{111}In-labeled antibodies retained their reactivity to the mesothelin antigen, suggesting that the radiolabeling procedure did not cause any major modification to the structure of the antigen-binding site. Saturation cell binding studies indicate that ^{111}In-mAbMB has a lower K_d and therefore a higher affinity for the mesothelin receptors as compared to ^{111}In-mAbK1 (Table 1). The number of mesothelin receptors on A431K5 cells, calculated from the B_{max} values was $6.3\times10^5\pm1.9\times10^5$ / cell.

3.3. Internalization by A431K5 cells

We studied internalization of ^{111}In-mAbMB and ^{111}In-mAbK1 from the cell membrane using A431K5 cells (Fig. 1). After a 1 h pre-incubation at 4°C (time 0 hours) 21.6±6.5% of total bound ^{111}In-mAbMB was present in the internalized acid resistant fraction, whereas for ^{111}In-mAbK1, the internalized fraction was only 6.0±2.5%. After 3 hours at 37°C, internalized fractions increased to 46.2±6.9% and 32.8±1.2% for ^{111}In-mAbMB and ^{111}In-mAbK1, respectively. After 6 hours, the internalized fractions were 52.1±3.7% and 41.5±7.6%, respectively. At 18 hours, the internalization of ^{111}In-mAbMB was significantly different ($P<.05$) at 76.4±6.8% compared to 59±0.6% for ^{111}In-mAbK1. Control studies carried out at 4°C showed that the internalized fraction increased slowly over time; at 18 hours maximal internalization of 29.9±10.0% and

Table 1
Immunoreactivity of ^{111}In-mAbMB and ^{111}In-mAbK1 determined by a cell-binding assay using A431K5 cells

	Immunoreactivity (%)	K_d (nM)
^{111}In-mAbMB	78.5±3.5	3.6±1.7
^{111}In-mAbK1	76.3±3.8	29.3±2.3

Total binding of ^{111}In-mAbMB and ^{111}In-mAbK1 to A431K5 cells was used to calculate K_d. Data is presented as mean±SD.

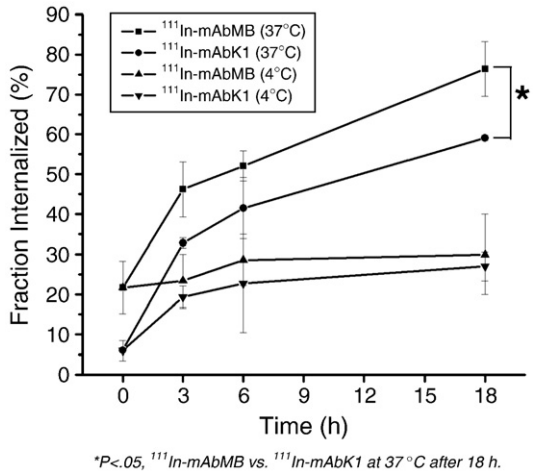

Fig. 1. Time and temperature dependent cellular internalization of ^{111}In-mAbMB and ^{111}In-mAbK1 by A431K5 cells. ^{111}In-mAbMB has greater cellular internalization than ^{111}In-mAbK1 throughout the time course of the study, with significantly higher values (P<.05) achieved at 18 hours. Data is presented as mean±SD.

26.9±3.6% was obtained for ^{111}In-mAbMB and ^{111}In-mAbK1, respectively.

3.4. Biodistribution studies

Biodistribution studies for ^{111}In-mAbMB were performed in SCID mice at two different doses. At the dose of 740 kBq (Fig. 2), after 24 hours, 8.74±3.25% ID/g was localized in the A431K5 tumors, whereas 4.5±0.91% ID/g was present in A431 tumors. Maximal A431K5 tumor uptake of 9.65±2.65% ID/g was obtained at 48 hours, which was significantly different (P<.05) from the corresponding uptake for A431 tumors, 4.7±1.65% ID/g. Thereafter, the tumor localization declined to <5% for A431K5 tumors and <3.5% for A431 tumors at 72 hours and remained steady until 96 hours. In addition to the tumors, ^{111}In-mAbMB showed uptake in the spleen, liver and kidneys. Spleen uptake was 82.4±15.3% ID/g after 24 hours and declined to 57.32±18.19% ID/g at 48 hours. Maximal uptake of ^{111}In-mAbMB into liver (17.79±3.04% ID/g) as well as kidneys (8.7±0.82% ID/g) was obtained at 24 hours. Blood activity remained relatively low at all time points and showed a steady decline from 4.71±1.58% ID/g at 24 hours to 1.29±0.58% ID/g at 96 hours. The tumor to blood ratio was >1 at all time points, and increased over time from 24 hours to 96 hours (Table 2). Biodistribution studies in mice without any tumors indicated low uptake of ^{111}In-mAbMB in spleen (8.06±0.70% ID/g) and 6.13±0.60% ID/g in liver, while rest of organs showed similar activity uptake as the tumor bearing mice (Fig. 3).

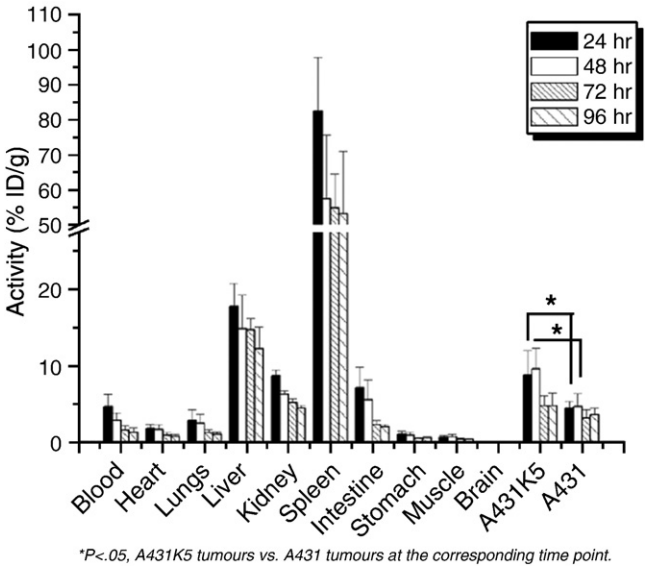

Fig. 2. Biodistribution of low dose ^{111}In-mAbMB (740 kBq) injected into SCID mice (n=5) bearing A431K5 (mesothelin positive) and A431 (mesothelin negative) subcutaneous xenografts. Percentage of the injected dose/gram (Activity %ID/g) was determined in the tumors and all major organs after 24, 48, 72 and 96 hours. Significantly higher localization of ^{111}In-mAbMB was observed in A431K5 tumors compared to A431 tumors at 24 and 48 hours time points, while non-specific uptake was mainly seen in the spleen. Data is presented as mean±SD.

When 7.4 to 10.1 MBq of ^{111}In-mAbMB was injected, 13.15±6.37% ID/g had localized in A431K5 tumors at 48 hours, whereas, at the same time A431 tumors accumulated 3.71±1.79% ID/g (Fig. 4). At 72 hours, 14.29±6.18% ID/g and 4.93±2.84% ID/g was found localized in A431K5 and A431 tumors, respectively. Kidney uptake at 48 hours (11.60 ±2.10% ID/g) was higher than the uptake with the lower dose (740 kBq) of ^{111}In-mAbMB, but at 72 hours the kidney uptake at both doses was similar. The overall spleen uptake of ^{111}In-mAbMB expressed in terms of %ID/organ at the higher dose was lower than that observed at the lower dose for both 48 and 72 hour time points (Fig. 5A). The spleen weights showed a decrease of about 60% compared to the spleen weights obtained at lower dose (Fig. 5B). As a result,

Table 2
Organ to blood ratios of low dose ^{111}In-mAbMB (740 kBq), injected in SCID mice (n=5) bearing A431K5 (mesothelin positive) and A431 (mesothelin negative) subcutaneous xenografts

Organ	24 hrs	48 hrs	72 hrs	96 hrs
Blood	1	1	1	1
Heart	0.41±0.05	0.54±0.13	0.61±0.12	0.68±0.12
Lungs	0.64±0.15	0.83±0.19	0.82±0.11	0.89±0.19
Liver	4.52±2.27	5.73±2.87	10.94±4.60	10.70±4.30
Kidneys	2.15±0.85	2.36±0.76	3.86±0.05	3.91±1.26
Spleen	19.79±5.99	20.74±8.28	39.33±15.12	44.67±18.71
Intestine	1.58±0.32	1.88±0.60	1.66±0.68	1.72±0.44
Stomach	0.23±0.05	0.31±0.05	0.38±0.10	0.49±0.12
Muscle	0.15±0.01	0.25±0.04	0.30±0.04	0.33±0.08
Brain	0.03±0.01	0.04±0.01	0.04±0.05	0.05±0.01
A431K5 (meso +)	1.89±0.36	3.23±0.66	3.27±0.51	3.83±0.38
A431 (meso -)	1.03±0.28	1.52±0.27	2.14±0.46	2.95±0.58

Biodistribution was determined after 24, 48, 72 and 96 hours. Data is presented as mean±SD.

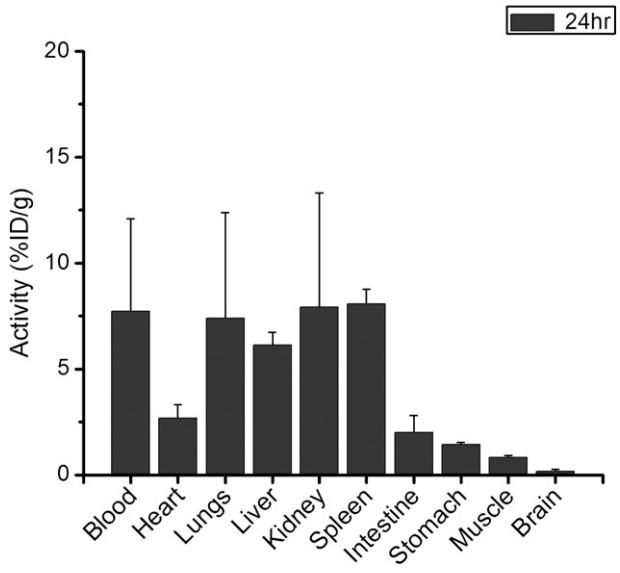

Fig. 3. Biodistribution of ^{111}In-mAbMB in mice without tumors (n=3). Percentage of the injected dose/gram (Activity %ID/g) was determined in all major organs after 24 hours. Data is presented as mean±SD.

the spleen activity in terms of % ID/g at the higher dose was greater than that observed at the lower dose for both 48 and 72 hour time points (Fig. 5C). Activity taken up by the liver was similar at both doses. Blood activity was 5.26±2.04% ID/g at 48 hours and further declined to 3.57±1.64% ID/g at

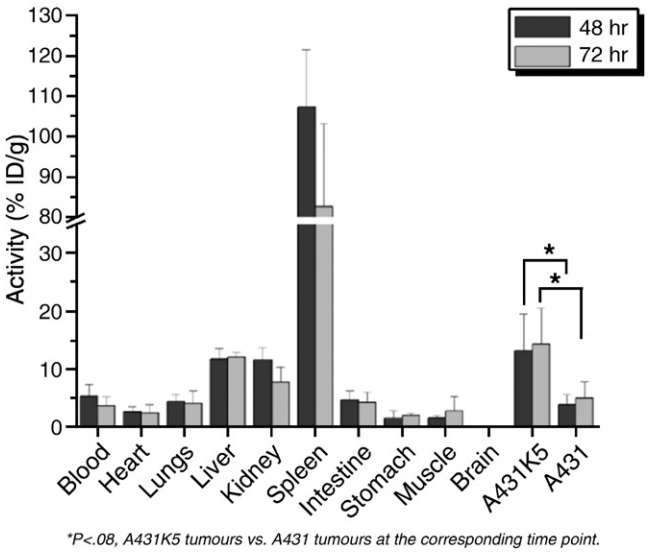

Fig. 4. Biodistribution of high dose ^{111}In-mAbMB (7.4 to 10.1 MBq), injected in SCID mice (n=3) bearing A431K5 (mesothelin positive) and A431 (mesothelin negative) subcutaneous xenografts. Percentage of the injected dose/gram (Activity %ID/g) was determined in the tumors and all major organs after 48 and 72 hours. Significantly higher localization of ^{111}In-mAbMB was observed in A431K5 tumors compared to A431 tumors at both time points, while non-specific uptake was mainly seen in the spleen. Data is presented as mean±SD.

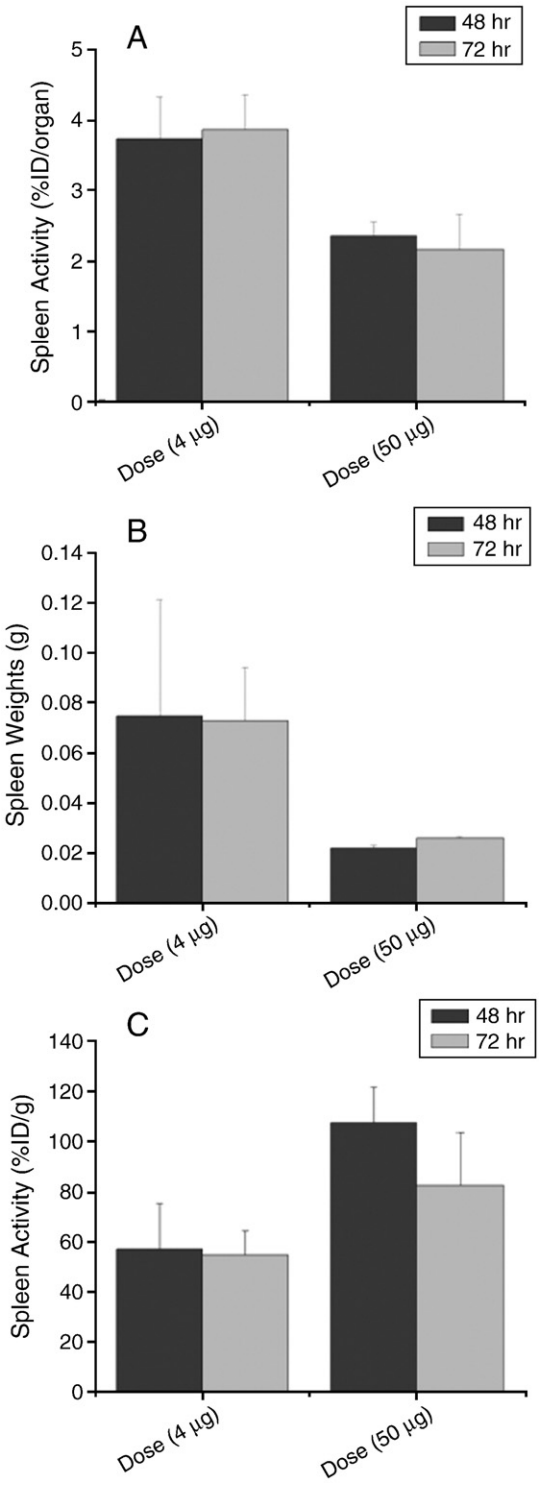

Fig. 5. A comparison of spleen activity uptake and spleen weights at 48 and 72 hours after injection of ^{111}In-mAbMB at low dose (4 µg) or high dose (50 µg). The spleen activity in terms of %ID/organ (A) decreases at the higher dose accompanied by decrease in the spleen weights (B), which results in an increased activity on per weight basis (%ID/g) in spleen (C). Data is presented as mean±SD.

Table 3
Organ to blood ratios of high dose ^{111}In-mAbMB (7.4 to 10.1 MBq), injected in SCID mice (n=3) bearing A431K5 and A431 subcutaneous xenografts

Organ	48 hrs	72 hrs
Blood	1	1
Heart	0.49±0.12	0.64±0.09
Lungs	0.86±0.11	1.08±0.12
Liver	2.42±4.60	3.84±1.52
Kidneys	2.37±0.05	2.25±0.30
Spleen	23.57±15.12	24.74±5.65
Intestine	0.90±0.68	1.18±0.26
Stomach	0.23±0.10	0.59±0.16
Muscle	0.31±0.04	0.64±0.37
Brain	0.03±0.05	0.06±0.02
A431K5 (meso +)	2.42±0.51	4.02±0.72
A431 (meso -)	0.68±0.46	1.43±0.80

Biodistribution was determined after 48 and 72 hours. Data is presented as mean±SD.

Table 4
Organ to blood ratios of ^{111}In-mAbK1 (740 kBq) in SCID mice (n=3) bearing A431K5 (mesothelin positive) and A431 (mesothelin negative) subcutaneous xenografts

Organ	24 hrs	72 hrs
Blood	1	1
Heart	1.08±0.14	3.39±0.61
Lungs	0.91±0.12	2.73±1.59
Liver	9.78±1.12	36.94±4.73
Kidneys	1.96±0.13	3.86±0.05
Spleen	3.26±0.47	11.80±1.60
Intestine	0.70±0.09	2.23±0.45
Stomach	0.55±0.09	2.53±1.44
Muscle	0.41±0.02	1.34±0.34
Brain	0.03±0.00	0.08±0.01
A431K5 (meso +)	1.20±0.26	5.29±0.88
A431 (meso -)	0.88±0.18	3.40±0.64

Biodistributions were determined after 24 and 72 hours. Data is presented as mean±SD.

72 hours. The maximal tumor to blood ratio of 4.02±0.72 was obtained for A431K5 tumors at 72 hours, while the corresponding tumor to blood ratio for A431 tumors was only 1.43±0.80 (Table 3).

For ^{111}In-mAbK1, biodistribution studies were carried out only at the dose of 740 kBq (Fig. 6). At 24 hours, 3.04±0.68% ID/g was taken up in the A431K5 tumors, while 2.22±0.41% ID/g was found in the A431 tumors. After 72 hours, tumor localization declined to 2.32±0.11% ID/g for A431K5 tumors and to 1.64±0.46% ID/g for A431 tumors. At both time points the activity uptake in the A431K5 tumors was significantly higher (P<.05) than in the A431 tumors. Liver uptake was 23.00±2.86% ID/g and 17.02±2.17% ID/g at 24 and 72 hours, respectively. Although the liver uptake was higher for ^{111}In-mAbK1 than ^{111}In-mAbMB, spleen showed much less uptake at both 24 (8.05±1.13% ID/g) and 72 hours (6.0±1.96% ID/g). ^{111}In-mAbK1 localization in the kidneys was 4.87±0.33 and 3.28±1.17% ID/g at 24 and 72 hours, respectively, which was again lower than that of ^{111}In-mAbMB. Blood activity was also lower (2.8±0.67% ID/g and 1.13±1.6% ID/g at 24 and 72 hours, respectively) indicating faster clearance of ^{111}In-mAbK1. At 24 hours, tumor to blood ratio for A431K5 tumors was 1.20±0.26, which increased to 5.29±0.88 after 72 hours (Table 4). The A431K5 tumor uptake of ^{111}In-mAbMB was significantly higher compared to uptake of ^{111}In-mAbK1 at both 24 hours (P=.005) and 72 hours (P=.002).

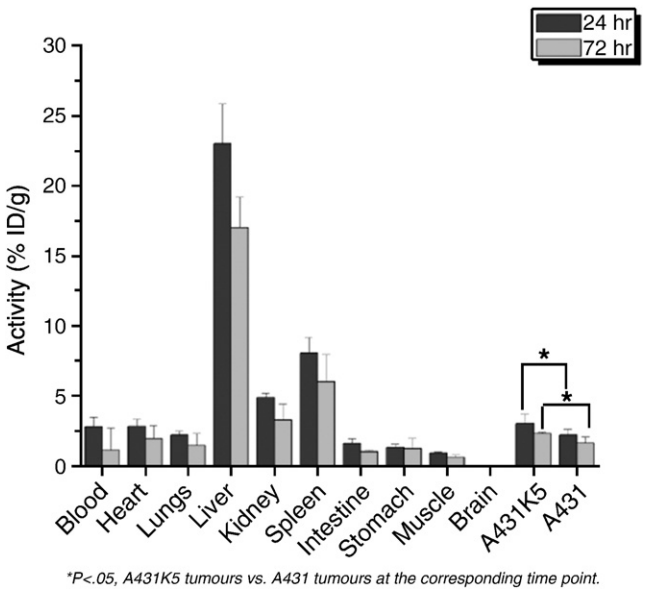

Fig. 6. Biodistribution of ^{111}In-mAbK1 (740 kBq), injected in SCID mice (n=5) bearing A431K5 (mesothelin positive) and A431 (mesothelin negative) subcutaneous xenografts. Percentage of the injected dose/gram (Activity %ID/g) was determined in the tumors and all major organs after 24 and 72 hours. Data is presented as mean±SD.

3.5. MicroSPECT/CT Imaging

^{111}In-mAbMB was clearly visualized in A431K5 tumors 24, 48 and 72 hours after injection (Fig. 7A). The activity distribution in spleen and liver was also evident, confirming the biodistribution studies. T/NT ratios for A431K5 and A431 tumors obtained by ROI analysis of the images showed that ^{111}In-mAbMB was targeted better to A431K5 tumors than to A431 tumors. The difference in T/NT ratios was significant at all the three time points (Fig. 8A). Although mice injected with ^{111}In-mAbK1 showed lower tumor uptake, the tumors were still visualized (Fig. 7B). ^{111}In-mAbK1 activity was also observed in the bladder indicating clearance through the organ. ROI analysis showed that A431K5 tumors had better uptake than A431 tumors, with T/NT ratios increasing over time (Fig. 8B), however statistical analysis was not carried out due to the small sample size. Better T/NT ratios and image contrast of A431K5 tumors was obtained for ^{111}In-mAbMB, compared to ^{111}In-mAbK1.

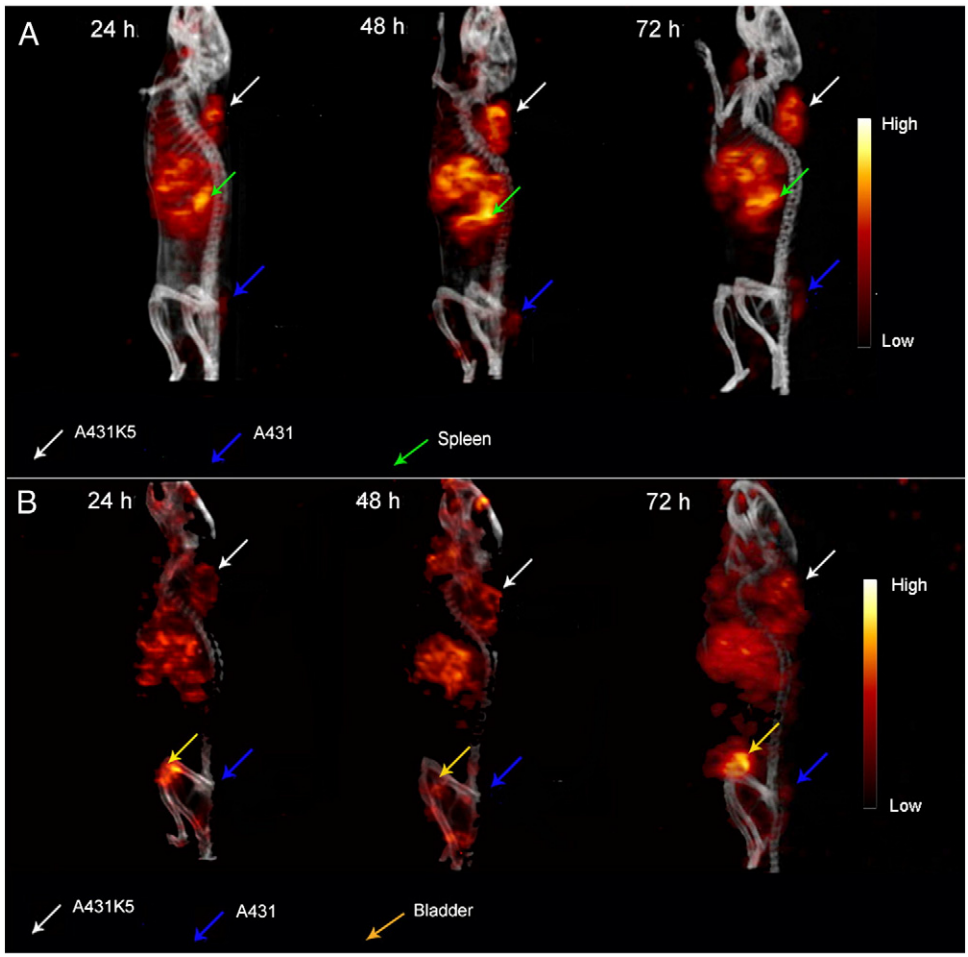

Fig. 7. MicroSPECT/CT images of SCID mice bearing A431K5 (mesothelin positive) and A431 (mesothelin negative) tumors. SCID mice were injected with 7.4 to 10.1 MBq of (A) ^{111}In-mAbMB and (B) ^{111}In-mAbK1 and images were acquired after 24, 48 and 72 hours, following anesthesia. The total counts/scan for 24, 48 and 72 hour acquisitions were 60,000-90,000, 45,000-65,000 and 40,000-50,000, respectively.

3.6. Mesothelin expression in tumors

Both A431K5 and A431 cells formed tumors following subcutaneous injection. Western blotting confirmed that mesothelin was expressed in the A431K5 tumors but not in the A431 tumors nor in the spleen (Fig. 9). Both the precursor (71 kDa) and mature mesothelin (40 kDa) bands were visualized on the Western blots.

4. Discussion

In the present study the preclinical SPECT imaging of mesothelin-expressing tumors using radiolabeled anti-mesothelin antibodies was successfully demonstrated. Although the tumor uptake with ^{111}In-mAbK1 was significantly lower than reported by Hassan et al., it was still possible to image the mesothelin-expressing tumors. In our studies, the observed superior uptake of ^{111}In-mAbK1 into A431K5 tumors, compared to previously observed uptake of ^{99m}Tc labeled mAbK1 in NCI-H226 tumors (unpublished data) can be attributed to the 7 times higher mesothelin expression by A431K5 cells (6.3×10^5 receptors/cell) than NCI-H226 tumors (9.1×10^4 receptors/cell; unpublished data). The mAbMB antibody was clearly superior in the form of the ^{111}In-mAbMB radioimmunoimaging bioprobe as revealed by the comparative studies to ^{111}In-mAbK1. In vitro studies also confirmed the specific binding and internalization of ^{111}In-mAbMB in mesothelin-expressing A431K5 cells. Such a radiolabeled antibody might be considered in patients, after applying recent strategies towards developing chimeric or fully humanized forms of this antibody [26].

Established cell lines such as NCI-H226 express low levels of mesothelin. For this reason, we used A431K5 cells which express mesothelin at levels similar to those seen on immunohistochemical examination of patient tumor specimens [27]. A431K5 cells are human, epidermoid A431 cells stably transfected with pcD3CAK1-9, a plasmid encoding the mesothelin gene [28]. Our studies indicate that A431K5 cells express about 6.3×10^5 mesothelin receptors per cell.

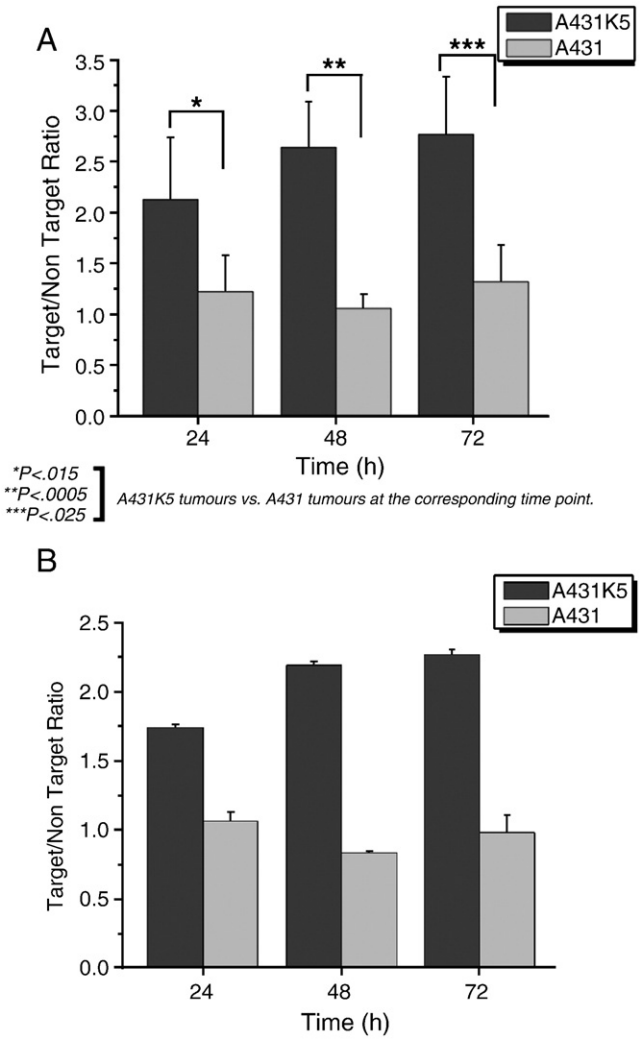

Fig. 8. Target to Non-Target (T/NT) ratios calculated from ROI analysis of microSPECT/CT images of SCID mice bearing A431K5 and A431 subcutaneous xenografts that were acquired (A) at 24 (n=6), 48 (n=6) and 72 (n=3) hours after injection with 7.4 to 10.1 MBq of ^{111}In-mAbMB and (B) at 24, 48 and 72 hours of mice (n=2) injected with 7.4 to 10.1 MBq of ^{111}In-mAbK1. Data is presented as mean±SD.

A requirement for a radiolabeled antibody is that it be able to bind a specific antigen with high affinity (low K_d). Under in vitro conditions, a K_d value between 10 pM (higher affinity) and 10 nM (lower affinity), is considered ideal [29]. We demonstrated that the affinity of ^{111}In-mAbMB (K_d=3.6 nM) for mesothelin receptors is about 8 times higher than that of ^{111}In-mAbK1 (K_d=29.3 nM). Onda et al. reported the same order of affinities using a surface plasmon resonance assay; they determined a K_d value of 0.6 nM for mAbMB whereas the K_d value was 12 nM for mAbK1. It is not clear why an earlier reported K_d value of 0.92 nM by the same group was many times lower, but it might explain why they saw such a high activity uptake (~53% ID/g) of ^{111}In-mAbK1 in mesothelin-expressing tumors in their studies [19]. Our studies indicate that the commercially

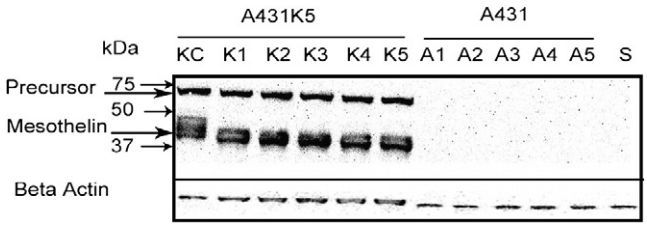

Fig. 9. Western blot confirmed mesothelin expression in A431K5 (K1-K5) tumors. The spleen (S) and A431 (A1-A5) tumors showed no expression of mesothelin. The cell lysate from A431K5 (KC) was used as a positive control, while beta actin was used as a loading control.

obtainable mAbK1 used by us has a much lower affinity than the antibody used in the study by Hassan et al.

Previous studies with A431K5 cells have demonstrated that mesothelin targeted immunoconjugates undergo internalization after binding to the cell surface [24,28]. Antibodies labeled with ^{111}In by means of a DTPA chelator can have an additional advantage in imaging if they become internalized by cells. Post internalization, ^{111}In is often trapped in the lysosomes of cells after catabolism of the antibody (residualization), thus leading to longer and higher retention inside the cells [30], which can help achieve higher target to non-target ratios. Our results showed that both ^{111}In-mAbMB and ^{111}In-mAbK1 are internalized by A431K5 cells. After 1 hour pre-incubation at 4°C, cellular internalization of ^{111}In-mAbMB was greater than that of ^{111}In-mAbK1, which further resulted in higher accumulation of ^{111}In-mAbMB in the cells over time. Imaging with ^{111}In-mAbMB, therefore, may be advantageous as its internalization was higher at all time points (Fig. 1). These results also indicate that mAbMB may be useful for radiotherapy when radiolabeled with a therapeutic radionuclide.

For unambiguous imaging, the radiolabeled antibody must accumulate at high levels within the tumors and be cleared from the blood within a time frame compatible with the radionuclide's half-life. Biodistribution studies at a dose of 4 μg/740 kBq of ^{111}In-mAbMB suggested that 24 to 72 hours is a good window for microSPECT/CT imaging (Fig. 2). While maximum uptake of ^{111}In-mAbMB into A431K5 tumors was obtained at 48 hours, the uptake into A431K5 tumors was significantly higher than A431 tumors at 24, 48 and 72 hours. Although the A431K5 tumor uptake of ^{111}In-mAbMB decreased at 72 hours, it was still significantly higher than uptake into A431 tumors (P=.002). At 96 hours, the uptake into A431K5 tumors was higher than A431 tumors, with a lower statistical difference (P=.08). The decreased levels of ^{111}In-mAbMB in A431K5 tumors at 72 and 96 hours can be attributed to two factors: 1) Shedding of antibody-bound mesothelin and its clearance from the A431K5 tumors and 2) possibility of some amount of ^{111}In-mAbMB being bound to free mesothelin antigen in the tumours, which can then undergo clearance from the tumours. However, more studies would be needed to investigate this.

The non-specific uptake of the radioactivity in A431 tumors is presumably a result of high vascular permeability, which leads to retention of activity by the Enhanced Permeation and Retention (EPR) effect [31]. ^{111}In-mAbMB was cleared from the blood at a fast rate resulting in steadily increasing tumor to blood ratios over time, which may also partially be an effect of residualization of ^{111}In in the tumors.

Since previous studies revealed that biodistribution and kinetics of radiolabeled antibodies can be dose dependent [32,33], we also investigated the post-imaging biodistribution at a higher antibody dose of 50 μg/9.25 MBq. Increasing the dose resulted in higher uptake at both 48 and 72 hours (Fig. 4). This increased accumulation in A431K5 tumors can partly be attributed to the availability of a higher dose of ^{111}In-mAbMB in the bloodstream due to about 30% lower non-specific accumulation (% ID/organ) in major sites such as liver and spleen.

Small amounts of mesothelin are expressed on the mesothelial lining of the lung and the peritoneal wall in normal mice with an expression pattern similar to that of humans [34]. Our biodistribution and imaging studies did not show any major uptake (cross-reactivity) by the lungs, as ^{111}In-mAbMB was cleared from the lungs at a similar rate as from blood. Also, little activity uptake was observed at these sites during imaging. At both doses activity was mainly localized in spleen and liver. Liver uptake is mostly a result of nonspecific dose contribution, as immunoglobulins from the bloodstream are trapped and processed there [33,35]. The observed high activity uptake by the spleen at the higher dose of ^{111}In-mAbMB was associated with decreases in spleen weights, which can be attributed to the depletion of hematopoietic cells resulting from higher radiation dose. Spleen being composed of lymphatic tissue is highly radiosensitive [36] and a loss of spleen weight in mice on exposure to radiation has been reported previously [37,38]. ^{111}In emits auger electrons in addition to the gamma radiation, which can cause toxic effects if taken up intracellularly due to local high density electron irradiation [39]. While it is known that the toxic auger effects depend on location of the radionuclide within the cell, the subcellular localization of ^{111}In-mAbMB in spleen needs further investigation. The percentage of injected dose in spleen when calculated on a per organ basis was lower at the 50 μg dose of ^{111}In-mAbMB compared to the 4 μg dose (Fig. 5A). However, the decrease in spleen weight (Fig. 5B) resulted in an apparent increase in percentage of injected dose on per gram basis in spleen (Fig. 5C). In addition to causing loss of spleen weight, spleen uptake can also interfere with the imaging of pancreatic tumors as the pancreas lies in close proximity to the spleen.

According to Bera et al. some expression of mesothelin may be expected in spleen [34], although we did not detect any using Western blotting (Fig. 9). Also, no cross reactivity of the mAbMB antibody towards proteins expressed by spleen was observed in the Western blot studies. Previously, Sato et al. have also reported high spleen uptake of their mesothelin targeted ^{111}In labeled tetravalent single-chain Fv-streptavidin fusion protein (SS1scFvSA), in mice bearing A431K5 tumors [24]. Although, the authors did not explain the reasons for the high spleen uptake, their results suggest a role of circulating mesothelin antigen in forming immune complexes with ^{111}In labeled SS1scFvSA, which then undergo phagocytic uptake by spleen. We believe that the spleen uptake of ^{111}In-mAbMB is mediated by a similar mechanism. Such a phenomenon is not predominant with ^{111}In-mAbK1 due to its lower affinity for mesothelin. We further investigated the possible role of circulating mesothelin antigen, by carrying out a biodistribution study in mice not bearing any tumors (Fig. 3). The low spleen and liver uptake of ^{111}In-mAbMB observed in these mice compared to tumor-bearing mice, clearly points to the role played by the shed tumor antigens in promoting spleen and liver uptake.

Although, we did not measure the amount of shed mesothelin in A431K5 tumor bearing mice, prior studies by Zhang *et al.* have shown that the amount of mesothelin shed into the blood circulation can range between 0.7 nM to 10 nM depending on the size of the A431K5 tumors. The presence of serum mesothelin has also been observed in mesothelioma and pancreatic cancer patients [40,41], but it remains to be seen whether it will lead to spleen uptake of ^{111}In-mAbMB in human patients. Prior studies in human patients injected with radiolabeled antibodies against carcinoembryonic antigen (CEA) have shown that although there is formation of immune complexes with the circulating antigens, the localization of activity into the tumors remains unaffected and there is no marked clearance of the radiolabel in the liver or the spleen. As a result, tumor detection by γ-immunoscintigraphy remained unaffected [42]. Nonetheless, if spleen uptake of ^{111}In-mAbMB is observed in human patients, pre-administration of unlabeled mAbMB may be used as a strategy to reduce the spleen uptake. The binding of unlabeled antibody mAbMB to the circulating mesothelin antigen would lead to its clearance from the circulation therefore preventing the formation of immune complexes with the subsequently administered ^{111}In-mAbMB. A similar strategy, involving pre-dosing of unlabeled anti-CD20 monoclonal antibodies to clear circulating CD20 positive B cells, followed by administration of ^{131}Iodine or ^{90}Yttrium labeled anti-CD20 monoclonal antibodies is currently being used in the clinic for radioimmunotherapeutic treatment of Non- Hodgkin's lymphoma [43]. Such a strategy would require optimal doses of unlabeled mAbMB antibody to be pre-administered, to prevent saturation of mesothelin receptors, prior to administration of ^{111}In-mAbMB. A pharmacokinetic modeling approach described previously can be used for dose optimization [44].

Our studies showed that the uptake of ^{111}In-mAbK1 into A431K5 tumors is much lower than that of ^{111}In-mAbMB, and is also very low compared to the high uptake reported by Hassan et al. [19]. We believe the main reason for this

disparity is the lower affinity of mAbK1 used in our studies. For tumor visualization, it is important to achieve a high tumor to surrounding tissue ratio together with high absolute activity uptake in the tumors. As seen in our SPECT/CT images, significant uptake of ^{111}In-mAbMB was detected in A431K5 tumors at all time points, which was much higher than that observed in A431 tumors and was consistent with the findings of the biodistribution studies (Fig. 4). The locations of high activity uptake were consistent over time and radiolocalization in the liver and spleen was also clearly resolved. As evident from the ROI analysis significantly higher T/NT ratios of ^{111}In-mAbMB were obtained for A431K5 tumors than A431 tumors at all time points (Fig. 8A). Although A431K5 tumors were visualized with ^{111}In-mAbK1, superior image contrast was obtained with ^{111}In-mAbMB.

5. Conclusion

We demonstrated that mesothelin expression can be imaged with SPECT in tumor-bearing mice using ^{111}In-labeled anti-mesothelin antibodies. The tumor uptake and imaging characteristics of ^{111}In-mAbMB make it a better choice than ^{111}In-mAbK1 for imaging mesothelin expression in tumors, although its non-specific uptake in spleen needs to be better understood and addressed. When fully optimized, such mesothelin-specific imaging agent will be useful in the diagnosis of mesothelioma, pancreatic cancer and ovarian cancer. Moreover, mesothelin targeting with therapeutic radioisotopes such as ^{90}Y, ^{188}Re, and ^{131}I or even the recently tested alpha-emitters ^{211}At and ^{213}Bi [33] can potentially be useful for radioimmunotherapy of tumors and their metastases [45].

Acknowledgments

We thank Chantal Saab, Dr. Troy Farncombe, and Rod Rhem at McMaster's Centre for Preclinical and Translational Imaging (Hamilton, Ontario, Canada) for excellent imaging support. We also thank John Humm from Memorial Sloan Kettering Hospital and Amin Kassis at Harvard Medical School for input into radiobiology questions. We appreciate support for this research from a Discovery Grant awarded to UOH by the Natural Sciences and Engineering Research Council of Canada (NSERC). RM is a recipient of the University Graduate Fellowship from the University of British Columbia.

References

[1] Wong HH, Lemoine NR. Pancreatic cancer: molecular pathogenesis and new therapeutic targets. Nat Rev Gastroenterol Hepatol 2009;6:412–22.
[2] Cubillos-Ruiz JR, Fiering S, Conejo-Garcia JR. Nanomolecular targeting of dendritic cells for ovarian cancer therapy. Future Oncol 2009;5:1189–92.
[3] Brand R. The diagnosis of pancreatic cancer. Cancer J 2001;7:287–97.
[4] Armato SG, Entwisle J, Truong MT, Nowak AK, Ceresoli GL, Zhao B, et al. Current state and future directions of pleural mesothelioma imaging. Lung Cancer 2008;59:411–20.
[5] Forstner R. Radiological staging of ovarian cancer: imaging findings and contribution of CT and MRI. Eur Radiol 2007; 17:3223–35.
[6] Goel A, Batra SK. Antibody constructs for radioimmunodiagnosis and treatment of human pancreatic cancer. Teratog Carcinog Mutagen 2001;21:45–57.
[7] Nock B, Nikolopoulou A, Chiotellis E, Loudos G, Maintas D, Reubi JC, et al. [^{99m}Tc]Demobesin 1, a novel potent bombesin analogue for GRP receptor-targeted tumour imaging. Eur J Nucl Med Mol Imaging 2003;30:247–58.
[8] Brader P, Kelly KJ, Chen N, Yu YA, Zhang Q, Zanzonico P, et al. Imaging a Genetically Engineered Oncolytic Vaccinia Virus (GLV-1h99) Using a Human Norepinephrine Transporter Reporter Gene. Clin Cancer Res 2009;15:3791–801.
[9] Yoshida C, Sogawa C, Tsuji AB, Sudo H, Sugyo A, Uehara T, et al. Development of positron emission tomography imaging by ^{64}Cu-labeled Fab for detecting ERC/mesothelin in a mesothelioma mouse model. Nucl Med Commun 2010;31:380–8.
[10] Tolmachev V. Imaging of HER-2 overexpression in tumors for guiding therapy. Curr Pharm Des 2008;14:2999–3019.
[11] Onda M, Willingham M, Nagata S, Bera TK, Beers R, Ho M, et al. New monoclonal antibodies to mesothelin useful for immunohistochemistry, fluorescence-activated cell sorting, Western blotting, and ELISA. Clin Cancer Res 2005;11:5840–6.
[12] Hassan R, Ho M. Mesothelin targeted cancer immunotherapy. European Journal of Cancer 2008;44:46–53.
[13] Argani P, Iacobuzio-Donahue C, Ryu B, Rosty C, Goggins M, Wilentz RE, et al. Mesothelin is overexpressed in the vast majority of ductal adenocarcinomas of the pancreas: identification of a new pancreatic cancer marker by serial analysis of gene expression (SAGE). Clin Cancer Res 2001;7:3862–8.
[14] Hassan R, Kreitman RJ, Pastan I, Willingham MC. Localization of mesothelin in epithelial ovarian cancer. Appl Immunohistochem Mol Morphol 2005;13:243–7.
[15] Muminova ZE, Strong TV, Shaw DR. Characterization of human mesothelin transcripts in ovarian and pancreatic cancer. BMC Cancer 2004;4:19.
[16] Scholler N, Garvik B, Hayden-Ledbetter M, Kline T, Urban N. Development of a CA125-mesothelin cell adhesion assay as a screening tool for biologics discovery. Cancer Lett 2007;247:130–6.
[17] Goldenberg DM. Targeted therapy of cancer with radiolabeled antibodies. J Nucl Med 2002;43:693–713.
[18] Chang K, Pastan I, Willingham MC. Isolation and characterization of a monoclonal antibody, K1, reactive with ovarian cancers and normal mesothelium. Int J Cancer 1992;50:373–81.
[19] Hassan R, Wu C, Brechbiel MW, Margulies I, Kreitman RJ, Pastan I. ^{111}Indium-labeled monoclonal antibody K1: biodistribution study in nude mice bearing a human carcinoma xenograft expressing mesothelin. Int J Cancer 1999;80:559–63.
[20] Rhodes BA, Martinez-Duncker C. Direct labeling of antibodies with ^{99m}Tc. Am Biotechnol Lab 1990;8:50–3.
[21] Hnatowich DJ, Childs RL, Lanteigne D, Najafi A. The preparation of DTPA-coupled antibodies radiolabeled with metallic radionuclides: an improved method. J Immunol Methods 1983;65:147–57.
[22] Lindmo T, Boven E, Cuttitta F, Fedorko J, Bunn Jr PA. Determination of the immunoreactive fraction of radiolabeled monoclonal antibodies by linear extrapolation to binding at infinite antigen excess. J Immunol Methods 1984;72:77–89.
[23] McLarty K, Cornelissen B, Scollard DA, Done SJ, Chun K, Reilly RM. Associations between the uptake of ^{111}In-DTPA-trastuzumab, HER2 density and response to trastuzumab (Herceptin) in athymic mice bearing subcutaneous human tumour xenografts. Eur J Nucl Med Mol Imaging 2009;36:81–93.

[24] Sato N, Hassan R, Axworthy DB, Wong KJ, Yu S, Theodore LJ, et al. Pretargeted radioimmunotherapy of mesothelin-expressing cancer using a tetravalent single-chain Fv-streptavidin fusion protein. J Nucl Med 2005;46:1201–9.
[25] Loening AM, Gambhir SS. AMIDE: a free software tool for multimodality medical image analysis. Mol Imaging 2003;2:131–7.
[26] Pelat T, Hust M, Thullier P. Obtention and engineering of non-human primate (NHP) antibodies for therapeutics. Mini Rev Med Chem 2009;9:1633–8.
[27] Hassan R, Lerner MR, Benbrook D, Lightfoot SA, Brackett DJ, Wang QC, et al. Antitumor activity of SS(dsFv)PE38 and SS1(dsFv)PE38, recombinant antimesothelin immunotoxins against human gynecologic cancers grown in organotypic culture in vitro. Clin Cancer Res 2002;8:3520–6.
[28] Chowdhury PS, Viner JL, Beers R, Pastan I. Isolation of a high-affinity stable single-chain Fv specific for mesothelin from DNA-immunized mice by phage display and construction of a recombinant immunotoxin with anti-tumor activity. Proc Natl Acad Sci U S A 1998;95:669–74.
[29] Eckelman WC, Kilbourn MR, Mathis CA. Discussion of targeting proteins in vivo: in vitro guidelines. Nucl Med Biol 2006;33:449–51.
[30] Press OW, Shan D, Howell-Clark J, Eary J, Appelbaum FR, Matthews D, et al. Comparative metabolism and retention of iodine-125, yttrium-90, and indium-111 radioimmunoconjugates by cancer cells. Cancer Res 1996;56:2123–9.
[31] Maeda H, Wu JC, Sawa T, Matsumura Y, Hori K. Tumor vascular permeability and the EPR effect in macromolecular therapeutics: a review. Journal of Controlled Release 2000;65:271–84.
[32] Dijkers EC, Kosterink JG, Rademaker AP, Perk LR, van Dongen GA, Bart J, et al. Development and characterization of clinical-grade ^{89}Zr-trastuzumab for HER2/neu immunoPET imaging. J Nucl Med 2009;50:974–81.
[33] Nakamae H, Wilbur DS, Hamlin DK, Thakar MS, Santos EB, Fisher DR, et al. Biodistributions, myelosuppression, and toxicities in mice treated with an anti-CD45 antibody labeled with the alpha-emitting radionuclides bismuth-213 or astatine-211. Cancer Res 2009;69:2408–15.
[34] Bera TK, Pastan I. Mesothelin is not required for normal mouse development or reproduction. Mol Cell Biol 2000;20:2902–6.
[35] Couturier O, Supiot S, Degraef-Mougin M, Faivre-Chauvet A, Carlier T, Chatal JF, et al. Cancer radioimmunotherapy with alpha-emitting nuclides. Eur J Nucl Med Mol Imaging 2005;32:601–14.
[36] Congdon CC. The destructive effect of radiation on lymphatic tissue. Cancer Res 1966;26:1211–20.
[37] Kurnick NB, Nokay N. Changes induced in the mouse spleen by graded doses of total-body x-irradiation. Radiat Res 1962;17:140–4.
[38] Cobb LM, Butler SA. Treatment of the murine lymphoma A31 with intravenous, sterilized, 114mIn-loaded A31 cells. Radiother Oncol 1987;10:217–30.
[39] Hofer KG. Biophysical aspects of Auger processes. Acta Oncol 2000;39:651–7.
[40] Tajima K, Hirama M, Shiomi K, Ishiwata T, Yoshioka M, Iwase A, et al. ERC/mesothelin as a marker for chemotherapeutic response in patients with mesothelioma. Anticancer Res 2008;28:3933–6.
[41] Johnston FM, Tan MC, Tan Jr BR, Porembka MR, Brunt EM, Linehan DC, et al. Circulating mesothelin protein and cellular antimesothelin immunity in patients with pancreatic cancer. Clin Cancer Res 2009;15:6511–8.
[42] Pimm MV. Circulating antigen: bad or good for immunoscintigraphy? Nucl Med Biol 1995;22:137–45.
[43] Dillman RO. Radiolabeled anti-CD20 monoclonal antibodies for the treatment of B-cell lymphoma. J Clin Oncol 2002;20:3545–57.
[44] Kletting P, Meyer C, Reske SN, Glatting G. Potential of optimal preloading in anti-CD20 antibody radioimmunotherapy: an investigation based on pharmacokinetic modeling. Cancer Biother Radiopharm 2010;25:279–87.
[45] Waldmann T. ABCs of radioisotopes used for radioimmunotherapy: alpha- and beta-emitters. Leuk Lymphoma 2003;44(Suppl 3): S107–13.